Applied Physics Express 7, 063001 (2014)
http://dx.doi.org/10.7567/APEX.7.063001

# Angular tunable zero-field ferromagnetic resonance frequency in oblique sputtered CoFeBSm thin films

Guozhi Chai[1,2*], Nguyen N. Phuoc[1], and Chong Kim Ong[3]

[1]*Temasek Laboratories, National University of Singapore, Singapore 117411*
[2]*Key Laboratory for Magnetism and Magnetic Materials of the Ministry of Education, Lanzhou University, Lanzhou 730000, P. R. China*
[3]*Center for Superconducting and Magnetic Materials, Department of Physics, National University of Singapore, Singapore 117542*
E-mail: chaigzh@lzu.edu.cn

Received March 12, 2014; accepted April 18, 2014; published online May 12, 2014

We investigated the high-frequency magnetic properties of oblique-sputtered CoFeBSm thin films. We found that the zero-field ferromagnetic resonance frequency $f_r$ can be tuned from 3.8 to 6.4 GHz by rotating the samples within the plane. The angular tunable $f_r$ is tentatively explained with the competition of uniaxial anisotropy (arising from the oblique deposition) the rotatable anisotropy (originating from the rotatable stripe domain). These results may have great implications for tunable microwave magnetic devices. © 2014 The Japan Society of Applied Physics

Magnetic thin films with tunable microwave magnetic properties are very useful for tunable microwave signal-processing devices, including tunable inductors, tunable resonators, phase shifters, and tunable filters.[1)] Conventional tunable microwave magnetic devices are tuned by using bulky, noisy, and power-consuming electromagnets with a magnetic field applied over the thin film to change the microwave magnetic properties. This deployment has a critical drawback that restricts its usage in most low-power-consumption and portable devices. One solution is to integrate the magnetic devices into electronic devices by using magnetoelectric (ME) coupling in multiferroic materials.[1)] Up to now, electrostatic tuning of the ferromagnetic resonance (FMR) frequency has been achieved in magnetic-ferroelectric films. Significant tuning of FMR frequency over a wide band can only be achieved in materials with especially large piezoelectric coefficients and large saturation magnetostriction constant.[1)] Thus, challenges still exist for tuning the FMR of thin films over a wide band for devices. An easy way to do this is to find materials that make up magnetic thin films whose FMR frequency can be tuned simply, without any external magnetic or electric field. It is well known from the Kittel equation[2)] that the FMR frequency is strongly dependent on anisotropy and the saturation magnetization $4\pi M_s$ in the films. In order to control the FMR frequency in magnetic thin films by changing the magnetic anisotropy, methods involving in situ depositing on pre-stressed substrates,[3)] exchange bias,[4)] multilayer structure[5,6)] and oblique deposition[7)] have been developed. However, most of these methods control the conditions during deposition, and these properties are impossible to change once the thin films have been used in devices. Rotatable anisotropy, whose direction can only be rotated by a large saturating field,[8,9)] is a candidate to achieve tunable FMR frequency in the magnetic thin films. Rotatable anisotropy was discovered many years ago, mainly in two kinds of magnetic thin films: ferromagnetic–antiferromagnetic (FM–AF) exchange-biased systems[8,9)] and thin films with stripe domains.[10,11)] Very recently, rotatable anisotropy has also been found in FM-doped ferrite thin films,[12–14)] with FM–ferrimagnetic exchange coupling, which is in principle quite similar to the FM–AF exchange-biased system, and may thus be placed into the first category.[12)] Thus, combining the uniaxial anisotropy and rotatable anisotropy may be a feasible way to tune the FMR frequency in magnetic thin films.

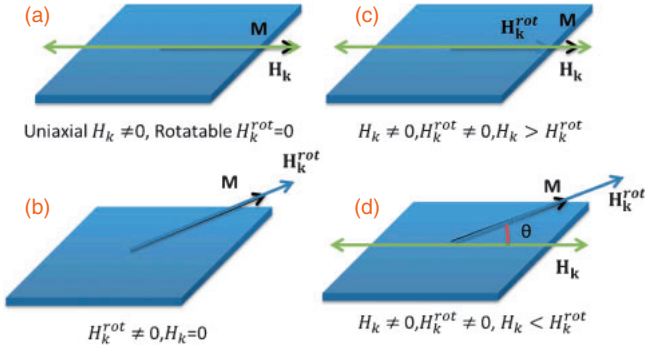


**Fig. 1.** Sketch of the stable magnetization direction in thin films with both rotatable anisotropy and uniaxial anisotropy.

Based on the Kittel equation,[2)] when the in-plane effective anisotropy is much less than the saturated magnetization, the resonance frequency of magnetic thin films can be written as

$$f_r \approx \frac{\gamma}{2\pi}\sqrt{H_k^{eff} \times 4\pi M_s}. \quad (1)$$

Only two types of magnetic anisotropies occur in these thin films: one is the rotatable anisotropy $H_k^{rot}$ and the other is the uniaxial anisotropy $H_k$. This leads to four possible cases: (1) thin film with uniaxial anisotropy only, without external field: in this case, the magnetization will lie in the same direction with the anisotropy, as shown in Fig. 1(a); (2) thin film with rotatable anisotropy only: in this case, as rotatable anisotropy rotates with the applied saturating magnetic field, which should be in the same direction as the remanant magnetization, and after removing the applied field, the magnetization should also lie in the same direction as the anisotropy, as shown in Fig. 1(b); (3) thin film with both types of anisotropies, and $H_k > H_k^{rot}$, without external field: as the uniaxial anisotropy is large enough to rotate the rotatable anisotropy, the rotatable anisotropy should rotate into the same direction as the uniaxial anisotropy and the magnetization should thus also lie in the same direction with the uniaxial anisotropy, as shown in Fig. 1(c); (4) thin film with both types of anisotropies, and $H_k < H_k^{rot}$, without external field: as the uniaxial anisotropy is not large enough to rotate the rotatable anisotropy, the magnetization should lie in the same direction as the rotatable anisotropy, which is different from the direction of uniaxial anisotropy, as shown in Fig. 1(d). For cases (1)–(3), the easy axis of the uniaxial

anisotropy and rotatable anisotropy lie in the same direction and Eq. (1) can thus be rewritten as

$$f_r \approx \frac{\gamma}{2\pi}\sqrt{(H_k + H_k^{rot}) \times 4\pi M_s}. \quad (2)$$

In these cases, the resonance frequency will remain constant once the thin films have been prepared without an external applied field. Only for case (4), the easy-axis directions of the two types of anisotropies are different; consequently the equation should be rewritten as

$$f_r \approx \frac{\gamma}{2\pi}\sqrt{(H_k \cos 2\theta + H_k^{rot}) \times 4\pi M_s}, \quad (3)$$

where $\theta$ is the angle between the two easy-axis directions of the anisotropies. In this case, the uniaxial anisotropy is fixed once the thin film has been prepared and the resonance frequency thus shows an angular dependence on the change of the easy axis direction of the rotatable anisotropy. In other words, the magnitude of the resonance frequency can be tuned by changing the direction of the rotatable anisotropy of the films by applying a saturating field.

As mentioned above, rotatable anisotropy can be formed in thin films with stripe domains,[10,11] FM–AF exchange-biased systems,[8,9] and with strong exchange-coupling systems.[12–14] Rotatable anisotropy in FM–AF systems is normally much smaller than the exchange bias field, which cannot rotate freely after removing the applied field., thin films with rotatable stripe domain structures or strong exchange coupling are the candidates for angularly tuning the resonance frequency by rotating the direction of the rotatable anisotropy. In this work, we select B and the rare-earth element Sm as dopants for FeCo films. B and Sm were used to reduce the grain size, and the in-plane uniaxial anisotropy of the films can be induced more easily.[15] The value of the anisotropy can be adjusted by oblique deposition.[7] The films are designed to be 180 nm thick, which is higher than the critical thickness, to obtain the rotatable stripe-domain structure.

180-nm-thick $Co_{37.2}Fe_{55.3}B_{4.9}Sm_{2.6}$ (CFBS) thin films with were deposited onto Si substrates with the radio frequency (RF) magnetron sputtering method. A radio frequency (RF) magnetron sputtering chamber was used to deposit 180-nm-thick CFBS magnetic thin films at ambient temperature onto $5 \times 10 \times 0.50\,mm^3$ Si(100) substrates, with a background pressure lower than $5 \times 10^{-7}$ Torr. A 3-in. $Co_{28}Fe_{67}B_5$ target with several attached equal-sized Sm chips was used, and the compositions of the magnetic thin films were controlled by changing the number of Sm chips. Some samples were deposited with different oblique incidence angles to induce uniaxial anisotropy with different magnitudes. During the sputtering process, an Ar flow rate of 16 sccm was kept constant to maintain an Ar pressure of $2 \times 10^{-3}$ Torr, and the RF power density was $2.7\,W/cm^2$. The thickness of the thin film was controlled both by the deposition time and by maintaining a constant deposition rate, which was verified with a thickness profile meter. The composition of the films was determined with an energy-dispersive X-ray spectroscope (EDS). The crystalline structure was studied by X-ray diffraction (XRD). Static magnetic properties of the films were characterized with a magnetic force microscope (MFM) with a soft magnetic tip and with a vibrating-sample magnetometer (VSM). Dynamic permeability spectra were measured

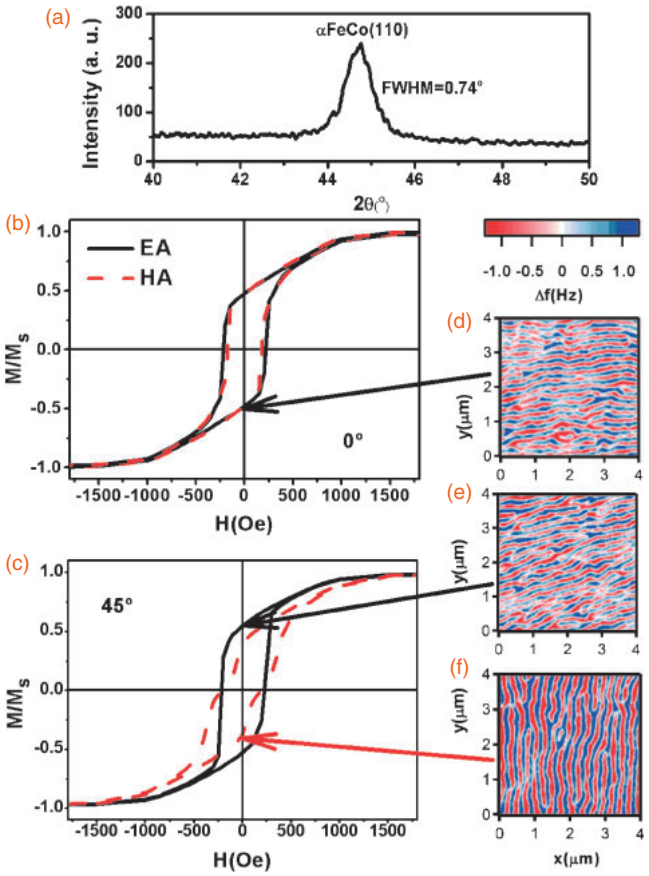


**Fig. 2.** (a) XRD results for CoFeBSm thin films; the main peak of CoFe [(110) peak of bcc structure] is observed in CoFeBSm thin films. The *M–H* loops of the CFBS magnetic thin films, (b) normal-deposited and (c) oblique-deposited with angle 45°. The dark solid lines were measured along the easy axis direction with maximum remanent magnetization, marked as EA, and the dashed red lines were taken along the perpendicular direction of the easy axis direction, marked as HA. MFM images of (d) normal-deposited and (e) and (f) oblique-deposited CFBS thin films.

with a vector network analyzer (VNA) using the room-temperature-shorted microstrip transmission line method[16] in conjunction with the near-field-microwave microscope (NFMM) method from 500 MHz to 10 GHz.[17] The angular dependence of high-frequency magnetic properties was measured with NFMM by attaching the thin films to an angular-resolved sample holder.

The CoFeBSm thin films are basically nanocrystalline thin films with grain sizes around 15.0 nm, calculated from the XRD pattern shown in Fig. 2(a). The static magnetic properties present in the *M–H* loops of CFBS thin films grown by conventional and oblique deposition methods are shown in Figs. 2(b) and 2(c). The *M–H* hysteresis loops were taken along different directions of the films to clearly reveal the magnetic anisotropic behavior of the films. The easy axis, marked with EA in the figure, corresponds to the *M–H* loop taken in-plane with the largest remanent magnetization, while the *M–H* loop taken perpendicularly to the EA but still in the plane of the film is defined as the hard axis (HA). As shown in Fig. 2(b) for the conventionally deposited films, practically no difference between the HA loop and the EA loop is evident, indicating that the magnetic properties of the films are almost isotropic within the plane. Moreover, the shapes of the loops which are of a typical shape for thin films with

stripe-domain structures imply that these thin films may possess weak perpendicular anisotropy, with some spins of the films aligned out of the film plane.[10,11] This argument is supported by the MFM images that show clear stripe domain structures as in Figs. 2(d)–2(f) for the CFBS thin films in the remanent state. In the MFM images, the color code represents the $\Delta f$ value, which indicates the magnitude of the z-component (i.e., perpendicular component) of the magnetization in the films (a positive $\Delta f$ value means that the magnetization points upward while a negative $\Delta f$ indicates that the magnetization points downward). Comparing with Figs. 2(e) and 2(f), the directions of the stripe domains can be rotated with an applied saturating field, which means that the domains can be rotated by an applied field. This follows from our knowledge that the easy axis of rotatable anisotropy will rotate with the domain wall direction. Thus, in these thin films with rotatable stripe domains, the rotatable anisotropy can be achieved with rotatable domain structures.[10] For films fabricated using an oblique deposition technique, the *M–H* loops shown in Fig. 2(c) are different from the ones for films fabricated without oblique deposition [Fig. 2(b)], in the sense that the remnant magnetization at HA is smaller than that of EA, which is indicative of anisotropic behavior. In addition, as in Figs. 2(e) and 2(f), the MFM images of this film taken at the remnant states after saturation at EA and HA are also of different colors, which means that the magnitudes of the perpendicular component in these films are different from the ones for films fabricated without oblique deposition. This result may be caused by the presence of uniaxial anisotropy from the oblique deposition technique, which is similar to the results for other oblique-deposited magnetic thin films.[7] Hence, in these CFBS thin films, we created a system that possesses both rotatable stripe domain structures and uniaxial magnetic anisotropy.

Figures 3(a) and 3(b) present dynamic permeability spectra with the imaginary parts ($\mu''$) of the films. The permeability spectra are measured along both the easy axis (a) and the hard axis (b) after saturation. The variation of the resonance frequency $f_r$ of the CFBS with the oblique deposition angle is shown in Fig. 3. The resonance frequency at the easy axis increases slightly from 5.3 to 6.4 GHz as the oblique deposition angle increases. However, the resonance frequency measured along the hard axis decreases from 5 to 3.8 GHz as the oblique deposition angle increases. Of interest is how the resonance frequency measured along different directions shows varying behaviors, which implies that the resonance frequency can be tuned from 3.8 to 6.4 GHz by rotating the magnetic thin films after saturation.

In order to yield insight into the angular behavior, we performed an investigation of the angular dependence of the high-frequency permeability spectra of these films.[18] This investigation was carried out by using a homemade, angular-resolved NFMM on VNA,[12,13,17] and the data is shown in Fig. 4. A typical result for the CFBS thin film deposited with an oblique angle of 31° is shown in Fig. 4(a). The variation in $f_r$ measured at different orientations after saturation indicates that the resonance frequency of the film can be tuned by rotating the sample. This angular-dependent experimental data for $f_r$ can be fitted to Eq. (3), and the fitting result for this thin film can be found in Fig. 4(b). We note that some discrepancy remains between the experimental data and the theoretical fitting curve, especially around the easy axis of the thin films. This behavior may be caused by dispersion of the magnetic anisotropy. Note that for the sake of simplicity in the model we used for our fitting, we ignore the dispersion of the magnetic anisotropy that may possibly occur in the films. For comparison, we plot the fitting results for CFBS thin films deposited without an angle and with an oblique angle of 45° in Figs. 4(c) and 4(d), respectively. For the films without oblique deposition, the small variation in $f_r$ indicates that the high-frequency responses of the films are nearly isotropic. However, larger variation of $f_r$ was found in the oblique-deposited CFBS film with an angle of 45°, which is caused by the presence of stronger uniaxial anisotropy.

By fitting the high-frequency permeability spectra with the LLG equation,[19] we can obtain the $H_k^{dyn}$ of the magnetic thin films, and from that value we can separate the rotatable anisotropy and uniaxial anisotropy by fitting the experimental data with Eq. (3). The magnitudes of the rotatable anisotropy and uniaxial anisotropy of the films with varying oblique angle are shown in Fig. 5. Note that the thicknesses and the

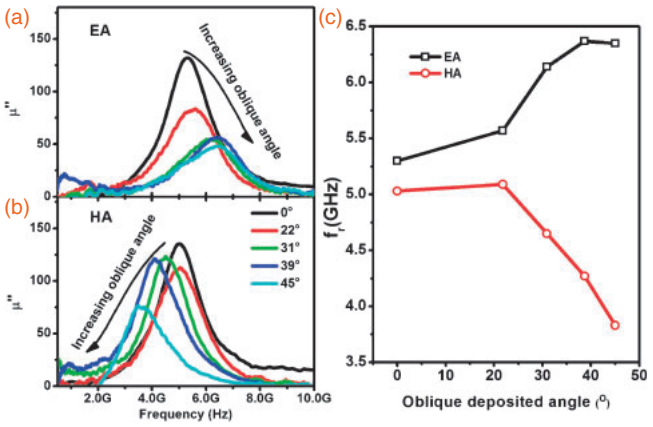


**Fig. 3.** The imaginary part of the permeability spectra of CFBS thin films measured along the (a) easy axis and (b) hard axis. (c) Easy axis (black dots and line) and hard axis (red circles and line) resonance frequency dependence on the oblique deposited angle.

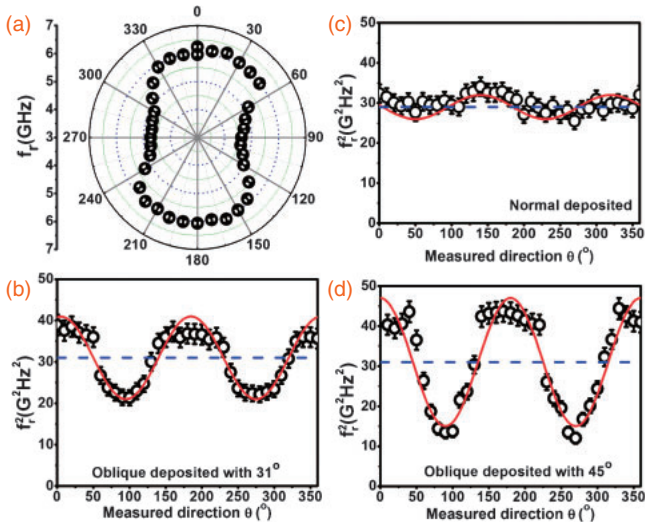


**Fig. 4.** (a) Angular dependence of the resonance frequency in oblique-deposited CFBS thin film with oblique angle 31°. The fitting curves and the experimental results of the angular dependence of the square of resonance frequency with oblique angle (b) 31°, (c) 0°, and (d) 45°.

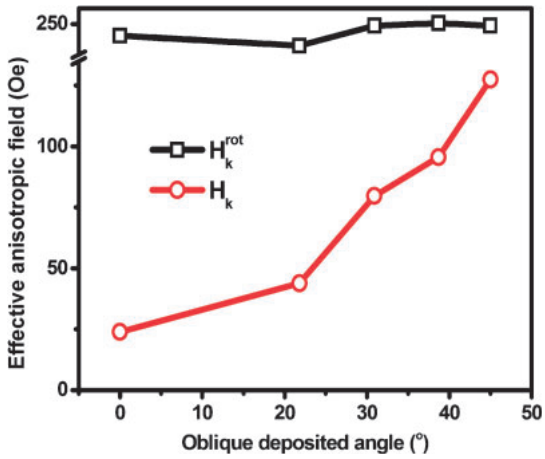


**Fig. 5.** The fitted magnitude of the rotational anisotropy (dark squares and black line) and uniaxial anisotropy (red circles and red line) of the oblique-deposited CFBS thin films, depending upon the oblique angle.

compositions of the thin films do not change, and thus the rotatable stripe domain size is not expected to change, as shown in Fig. 2. Hence, the rotatable anisotropy should remain constant as observed in Fig. 5, because it is driven by the rotatable stripe domain structure. The uniaxial anisotropy increases with increasing oblique angle, which is generally explained by the so-called self-shadow effect. This results in a tilted columnar structure of the grains and sometimes in elongated columns.[20)]

In summary, we report the development of CoFeBSm magnetic thin films with angular tunable resonance frequency. The angular tunable zero-field ferromagnetic resonance frequency in these films originates from two different types of anisotropy, an isotropic-rotatable anisotropy due to the rotatable stripe domains and a uniaxial anisotropy introduced by the oblique deposition. Our findings for this material suggest a method for tailoring the high-frequency properties of magnetic thin films, which should be useful for high-frequency applications.

**Acknowledgment** Dr. Chai thanks the financial support from National Natural Science Foundation of China (NSFC) (No. 51107055).

1) N. X. Sun and G. Srinivasan, Spin **2**, 1240004 (2012).
2) C. Kittel, Phys. Rev. **71**, 270 (1947).
3) Y. Fu, Z. Yang, T. Miyao, M. Matsumoto, X. X. Liu, and A. Morisako, Mater. Sci. Eng. B **133**, 61 (2006).
4) J. McCord, R. Kaltofen, O. G. Schmidt, and L. Schultz, Appl. Phys. Lett. **92**, 162506 (2008).
5) G. Z. Chai, Y. C. Yang, J. Y. Zhu, M. Lin, W. B. Sui, D. W. Guo, X. L. Li, and D. S. Xue, Appl. Phys. Lett. **96**, 012505 (2010).
6) G. Z. Chai, Z. L. Wang, G. X. Wang, W. B. Sui, and D. S. Xue, IEEE Trans. Magn. **47**, 3115 (2011).
7) W. D. Li, O. Kitakami, and Y. Shimada, J. Appl. Phys. **83**, 6661 (1998).
8) M. D. Stiles and R. D. McMichael, Phys. Rev. B **59**, 3722 (1999).
9) J. McCord, R. Mattheis, and D. Elefant, Phys. Rev. B **70**, 094420 (2004).
10) R. J. Prosen, J. O. Holmen, and B. E. Gran, J. Appl. Phys. **32**, S91 (1961).
11) G. X. Wang, C. H. Dong, W. X. Wang, Z. L. Wang, G. Z. Chai, C. J. Jiang, and D. S. Xue, J. Appl. Phys. **112**, 093907 (2012).
12) G. Z. Chai, N. N. Phuoc, and C. K. Ong, Sci. Rep. **2**, 832 (2012).
13) G. Z. Chai, N. N. Phuoc, and C. K. Ong, Appl. Phys. Lett. **103**, 042412 (2013).
14) G. Z. Chai, N. N. Phuoc, and C. K. Ong, J. Phys. D **46**, 415001 (2013).
15) K. Ikeda, T. Suzuki, and T. Sato, J. Magn. Soc. Jpn. **32**, 179 (2008).
16) Y. Liu, L. F. Chen, C. Y. Tan, H. J. Liu, and C. K. Ong, Rev. Sci. Instrum. **76**, 063911 (2005).
17) L. T. Hung, N. N. Phuoc, X. C. Wang, and C. K. Ong, Rev. Sci. Instrum. **82**, 084701 (2011).
18) R. Lopusnik, J. P. Nibarger, T. J. Silva, and Z. Celinski, Appl. Phys. Lett. **83**, 96 (2003).
19) T. L. Gilbert, IEEE Trans. Magn. **40**, 3443 (2004).
20) R. D. McMichael, C. G. Lee, J. E. Bonevich, P. J. Chen, W. Miller, and W. F. Egelhoff, Jr., J. Appl. Phys. **88**, 3561 (2000).